4. Additional considerations for moving observers

The relations discussed so far can easily be extended from two to several observers. Doing this, first the addition of velocities must be derived, because the relativistic case shows not the simple summation which could be expected according to the laws of the Galilei-Transformation. Further special relations exist in connection with velocities lower than the speed of light, which are observed e.g. concerning light in transparent media or connected with the transport of sound in solid bodies. These relations are also valid during acceleration of observers because material objects cannot be considered as absolute rigid.

In addition the case is discussed, when the transport of a signal inside a moving body is not only taking place in the direction of the movement but also transverse to it.

4.1 Relativistic addition of velocities

The theorem for the addition of velocities in the relativistic case was derived by A. Einstein already in the year 1905 [12]. It is assumed that in a system S′, which is moving with the speed v in direction of the x-axis in relation to the reference system S, an observer is moving according to the relations

$$x' = w_x' t' \tag{4.01}$$

$$y' = w_y' t' \tag{4.02}$$

$$z' = 0 \tag{4.03}$$

where w_x' and w_y' are the components of the velocity in x' resp. y'-direction. The aim is to find a relation referring to the reference system S. The coordinate system is selected in a way that all points are situated in the $x - y$ plane and so the coordinate z' can remain unconsidered.

Thus, the Lorentz equations read

$$x' = \gamma(x - vt) \tag{4.04}$$

$$y' = y \tag{4.05}$$

$$t' = \gamma\left(t - \frac{v}{c^2}x\right) \tag{4.06}$$

Behavior in x-direction

When Eq. (4.04) and Eq. (4.06) are inserted in Eq. (4.01) this yields

$$\gamma(x - vt) = w_x' \cdot \gamma\left(t - \frac{v}{c^2}x\right) \tag{4.07}$$

with

$$x = \frac{w_x' + v}{1 + \frac{vw_x'}{c^2}} \cdot t \tag{4.08}$$

Behavior in y-direction

For the determination equations Eq. (4.02), (4.06) and (4.08) are successively inserted in Eq. (4.05)

$$y = y' = w_y'\gamma\left(t - \frac{v}{c^2}x\right) \tag{4.09}$$

$$y = w_y'\gamma\left(t - \frac{v}{c^2} \cdot \frac{w_x' + v}{1 + \frac{vw_x'}{c^2}} \cdot t\right) \tag{4.10}$$

following

$$y = w_y'\gamma \frac{1 + \frac{vw_x'}{c^2} - \frac{vw_x'}{c^2} - \frac{v^2}{c^2}}{1 + \frac{vw_x'}{c^2}} \cdot t \tag{4.11}$$

$$y = \frac{\sqrt{1 - \frac{v^2}{c^2}}}{1 + \frac{vw_x'}{c^2}} w_y' t \tag{4.12}$$

Because of the linearity of the relations the velocities can be derived out of Eq. (4.08) and (4.12) in a simple way as

$$\frac{dx}{dt} = w_x = \frac{w_x' + v}{1 + \frac{vw_x'}{c^2}} \tag{4.13}$$

$$\frac{dy}{dt} = w_y = \frac{\sqrt{1 - \frac{v^2}{c^2}}}{1 + \frac{vw_x'}{c^2}} w_y' \tag{4.14}$$

In a final step the angles of the velocity-components in relation to the x-axis are inserted which yields

$$w'_x = w \cdot cos\,\alpha \tag{4.15}$$

$$w'_y = w \cdot sin\,\alpha \tag{4.16}$$

and by using

$$v_T = \sqrt{w_x^2 + w_y^2} \tag{4.17}$$

these are added as vectors

$$\sqrt{\left(\frac{w\,cos\,\alpha + v}{1 + \frac{v\,w\,cos\,\alpha}{c^2}}\right)^2 + \left(\frac{\sqrt{1 - \frac{v^2}{c^2}}}{1 + \frac{v\,w\,cos\,\alpha}{c^2}}\,w\,sin\,\alpha\right)^2} \tag{4.18}$$

For the total velocity v_T in system S and after transformation and using the general relation

$$cos^2\alpha + sin^2\alpha = 1 \tag{4.19}$$

the final solution is

$$v_T = \frac{\sqrt{v^2 + w^2 + 2\,v\,w\,cos\alpha - \left(\frac{v\,w\,sin\alpha}{c}\right)^2}}{1 + \frac{v\,w\,cos\alpha}{c^2}} \tag{4.20}$$

If the velocities v and w are situated unidirectional, which means angle $\alpha = 0$, then Eq. (4.20) is simplified to

$$v_T = \frac{v + w}{1 + \frac{v\,w}{c^2}} \tag{4.21}$$

When this situation concerning emitted signals and their reception is presented in a space-time diagram then the configuration in Fig. 4.1 is achieved. On the left side of this chart the situation is presented, that the emitter in the middle is belonging to a system at rest. The receivers of the signals, which are in addition reflecting the incoming signals immediately, are increasing their distance with equal speed (in this case: $v = w = 0{,}5c$). On the right-hand side, it is illustrated how the same situation develops from the view of an observer which was considered as in motion before (in this case: B). One of the observers is increasing the distance with the same speed of $v = 0{,}5c$, the third shows a speed of $v = 0{,}8c$ according to equation (4.21). A reverse situation develops when observer C is considered as at rest.

To illustrate the exact circumstances, the situation for times $t = 1$ TU and $t = 2$ TU are marked with different shades in the space-time diagram (Fig. 4.1). In this presentation it is clearly visible, that irrespective of the velocity of an observer always the same results will be achieved.

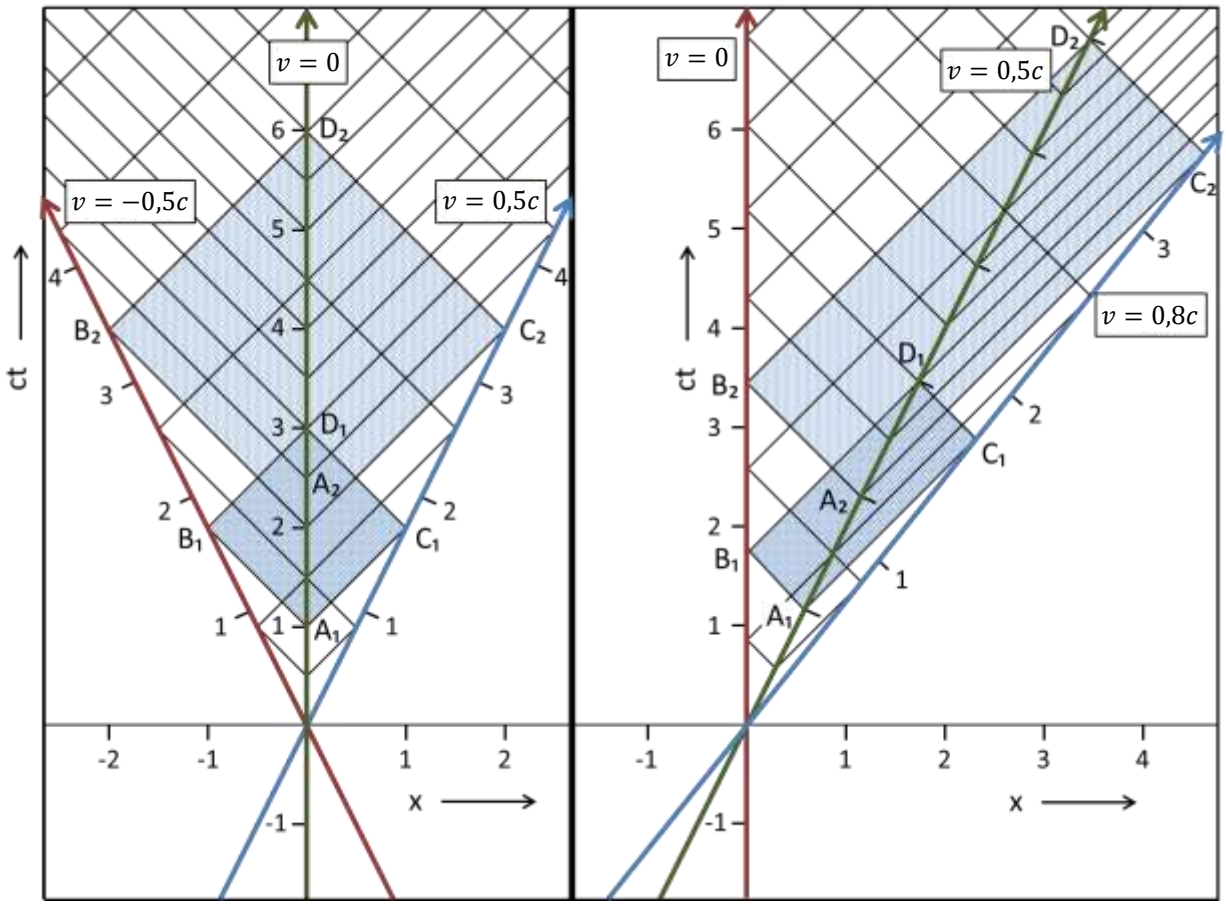

Fig. 4.1: Space-time diagram for observers at rest and in motion

4.2 Experiments with transparent media in motion

In the following a further alternative of the case discussed in chapter 2.2.2 will be looked at. Instead of a light pulse a second observer shall be shifted inside the body in moving direction and opposite to it. In conjunction with the exchange of light pulses the following combinations are possible:

A: Light pulse going and coming,

B: Observer in motion (in moving direction), light pulse comes back,

C: Light pulse going, observer in motion (opposite to moving direction),

D: Observer in motion (in moving direction and opposite).

In Fig. 4.2 possible combinations for the velocity of bodies in motion with $v = 0{,}5\ c$ are presented. As already shown, the velocities in the relativistic range are calculated according to Eq. (4.21). In this case of a system velocity of $v_1 = 0{,}5\ c$ and an additional velocity of a body in motion of also $v_2 = 0{,}5\ c$ was assumed and the result is $v_T = 0{,}8\ c$.

The figure shows clearly that the cases B and C, i.e. the combination of light pulse and body in motion, are leading to the same results.

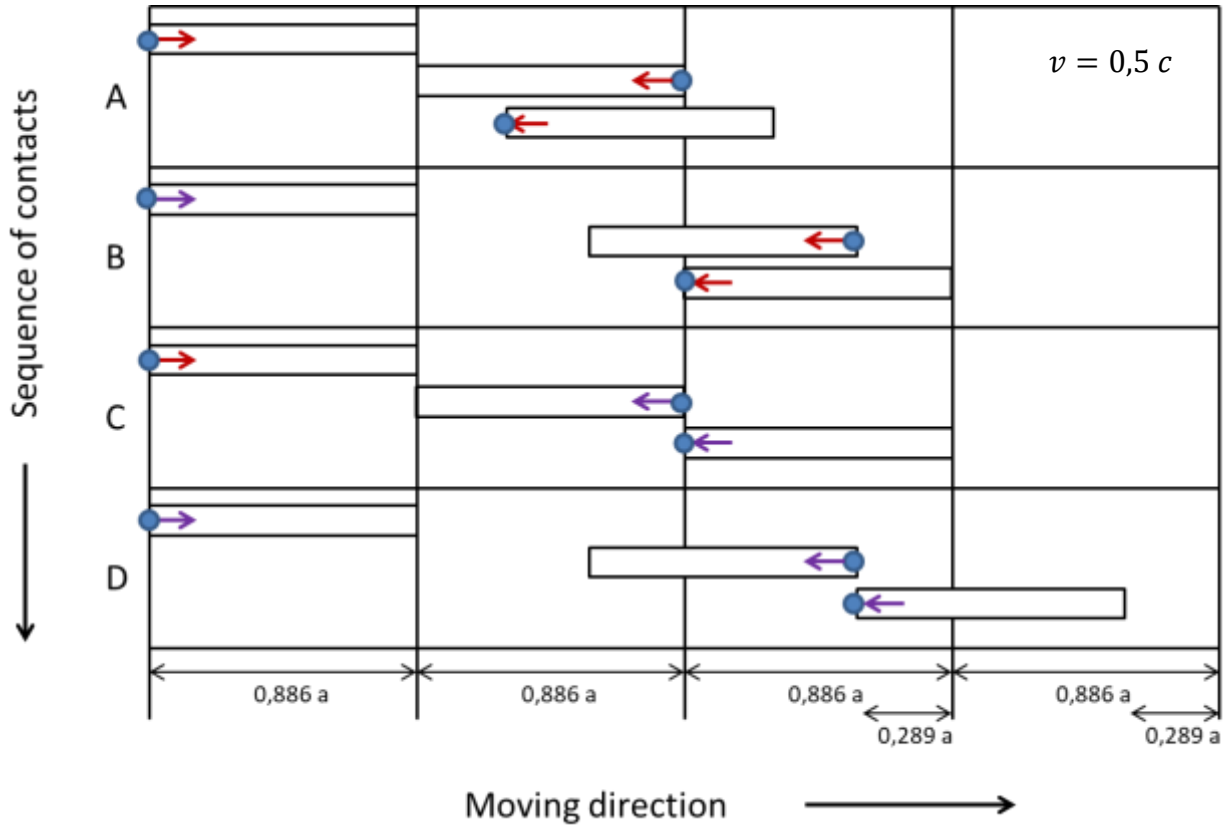

Fig. 4.2: Exchange of signals and bodies in motion in a moved system
A: Light pulse going and coming,
B: Body in motion (in moving direction), light pulse comes back,
C: Light pulse going, body in motion (opposite to moving direction),
D: Body in motion (in moving direction and opposite).

An experimental proof of these cases with bodies in motion is, however, only possible with extreme restrictions because of the high velocities needed. An experimental assessment is yet possible by an examination using optical tools. The speed of light c_n in media is defined as

$$c_n = \frac{c}{n} \tag{4.30}$$

with n as refractive index. It was already in the year 1812 that Augustin Jean Fresnel (1788-1827) developed the hypothesis, that the speed of light in moved media can be calculated by using a dragging coefficient (which was later named after him). According to this the speed of light in a moving system for an observer at rest is

$$c_T = \frac{c}{n} + v\left(1 - \frac{1}{n^2}\right) \tag{4.31}$$

This theory was verified in the year 1851 by Hippolyte Fizeau (1819-1896) with an experiment where he measured the speed of light in water which was flowing with different velocities. After the full development of the Lorentz-equations it was possible to show, that the addition of velocities of moved media and the light propagation c_n inside can be calculated using the addition of relativistic speed [36].

For calculation Eq. (4.21) is used

$$v_T = \frac{v_1 + v_2}{1 + \frac{v_1 v_2}{c^2}} \tag{4.32}$$

and with $v_1 = c_n$ this yield

$$v_T = \frac{\frac{c}{n} + v_2}{1 + \frac{v_2}{nc}} = \frac{c^2 + ncv_2}{nc + v_2} \tag{4.33}$$

A Taylor expansion for v_2 is leading to

$$v_T = \frac{c}{n} + v_2\left(1 - \frac{1}{n^2}\right) - \frac{v_2^2}{nc}\left(1 - \frac{1}{n^2}\right) + \frac{v_2^3}{n^2c^2}\left(1 - \frac{1}{n^2}\right) - + \ldots \tag{4.34}$$

This equation is, concerning terms of first order, equal to the relation given in equation Eq (4.31).

A calculation using the Lorentz-Transformation for the situation according to Fig 4.2 show the results presented in Tab. 4.1. In Fig 4.3 the results are presented in a diagram. As expected after the end of the experiment all values are located on the ct'- line. Furthermore, it is evident that the transformation equations confirm the expected relations and that no contradictions can be observed.

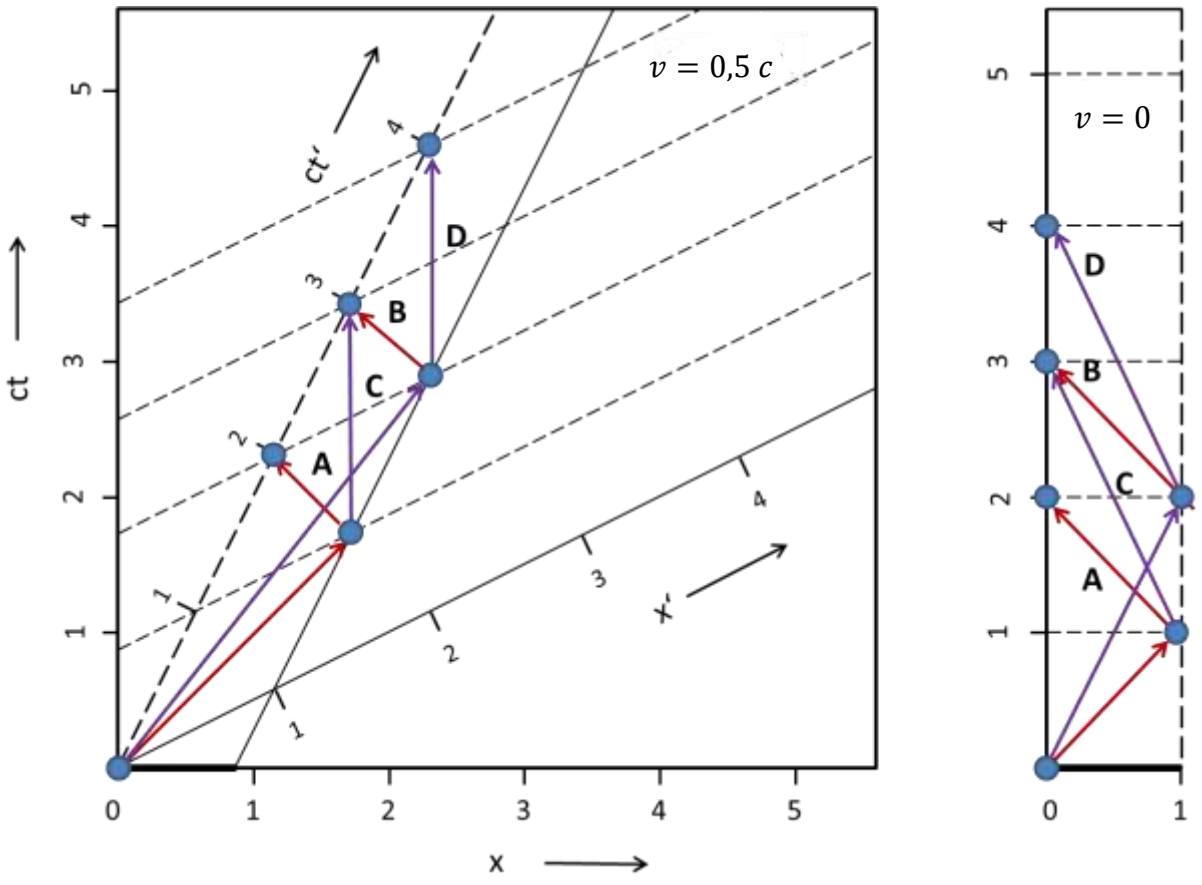

Fig. 4.3: Minkowski-diagram for cases A, B, C and D according to Fig. 4.2. Left: moved ($v = 0{,}5\ c$), right: at rest ($v = 0$)

Case	E_0	E_0'	E_1	E_1'	E_2	E_2'
A	[0;0]	[0;0]	[1,73;1,73]	[1;1]	[1,15;2,31]	[0;2]
B	[0;0]	[0;0]	[2,31;2,89]	[1;2]	[1,73;3,46]	[0;3]
C	[0;0]	[0;0]	[1,73;1,73]	[1;1]	[1,73;3,46]	[0;3]
D	[0;0]	[0;0]	[2,31;2,89]	[1;2]	[2,31;4,62]	[0;4]

Tab. 4.1: Calculated values for the situations presented in Fig. 4.2

The validity of this equation was verified in a multitude of experiments, first by H. Fizeau using flowing water and later e.g. by R. V. Jones using rotating transparent discs [37,38]. It is therefore an important part of physics and belongs both to the foundations of optics and relativistic considerations.

4.3 Triggering of engines after synchronization

It was already discussed in detail and demonstrated based on several examples that after mere kinematic considerations during the exchange of signals in laboratory systems after an "Einstein-Synchronization" no discrepancies will occur. A similar situation exists, when signals are used not only for synchronization of clocks but to trigger engines which influence the movement of the laboratory. The following situation shall be discussed:

1. From the middle of a laboratory signals are sent at the same time in different directions A and B.
2. When a signal is detected at A or B an engine will be started instantly in transverse direction compared to the direction of the incoming signal. The acceleration at A and B follow the same orientation.
3. Tests are executed in a situation at rest and in motion.

First, it is clear that A and B will start their engines at the same time when the laboratory is in a situation at rest (Fig. 4.4, right-hand side). This is not the case for a moved system, however. While the observer in motion after a previous synchronization realizes that the engines will start at the same time, an observer at rest will monitor that, because of the longer running time of the signal from the middle to A´ compared to B´, the engine at B´ will start first. Because of the acceleration transverse to the moving direction according to this consideration a momentum is generated, and the laboratory should start to turn.

In the literature cases like this are discussed quite often. A similar approach was examined by M. Born and during considerations of electrodynamics the assumption was made that an observer (here: the laboratory) with an unlimited rigidity would create discrepancies [39]. An unlimited rigidity (sometimes also called "Born's rigidity") cannot be valid, however, because all real material objects show a limited and not an infinite speed of sound which would be necessary for unlimited rigidity. The situation was discussed at length by A. Sommerfeld [15d].

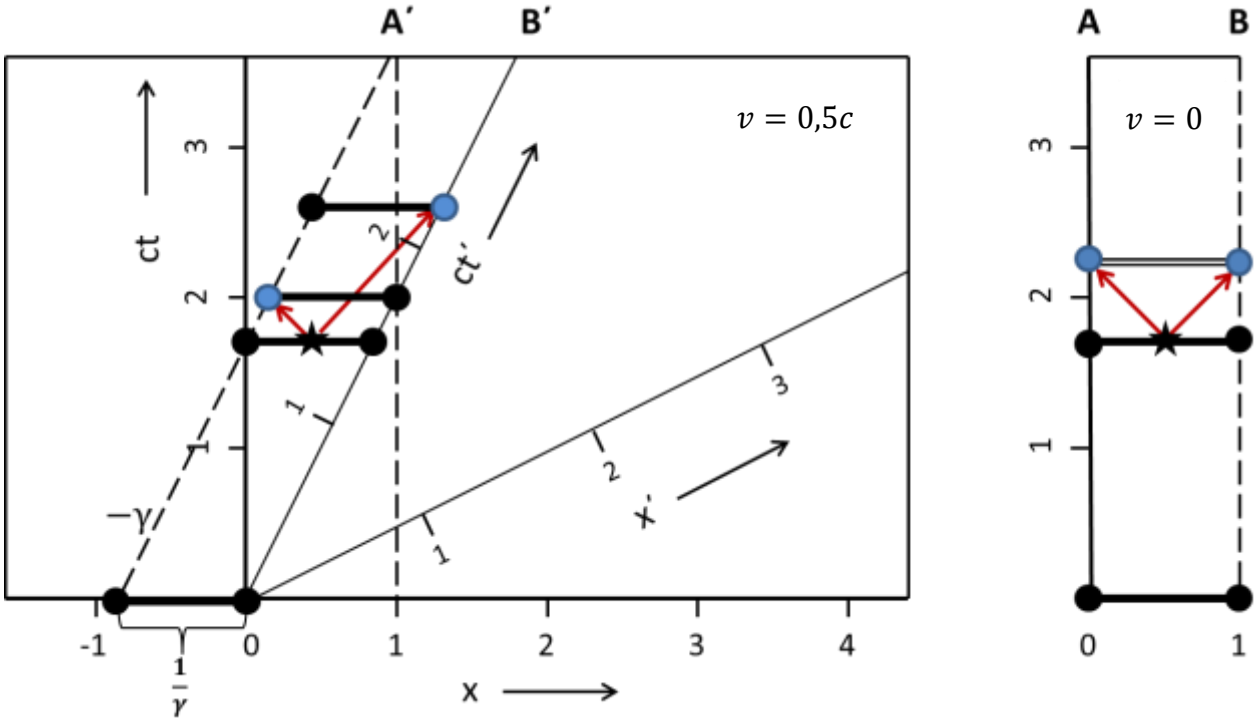

Fig. 4.4: Laboratory with signals to trigger an engine in transverse direction ($v = 0{,}5\ c$). Left: System in motion; Right: System at rest

If the situation is considered in a way that the propagation of a signal is using the speed of sound (or any other limited velocity up to the speed of light), the relativistic addition of velocities lead to the same case that was discussed in chapter 4.2. The propagation of the movements in transverse direction caused by the different engines will arrive at the same time in the middle of the laboratory and thus no momentum will be generated.

4.4 Exchange of signals between observers with spatial geometry

Up to now the exchange of signals between observers with an elongation in only one direction was discussed. To extend this for objects with spatial geometry, an experimental set-up like in chapter 2.2.2 is chosen with the difference, however, that for the laboratories objects with equilateral triangles were selected.

The signals are therefore not emitted longitudinal, but with an angle of 60° to this direction (see Fig. 4.5). When the observers in both systems pass each other at A, B, resp. A′ and B′ a signal is sent to C resp. C′. Both C and C′ are reflecting the signals back to the sender and the measured times are monitored. For an observer at rest the situation of a system in motion is defined as presented in Fig. 4.6. First, the base of the equilateral triangle with length a is shortened by the factor γ in moving direction, which is resulting in the effect that 4 cases for contacts between the corners of the triangles will occur. These situations are shown in the left-hand side of Fig. 4.6. Whereas inside the moving system the distance from A′ to C′ (cases 1 and 3) and B′ to C′ (cases 2 and 4) is subjectively viewed as shown (in the diagram presented with dotted lines), for the system at rest the way of the signal is following d as defined in the right-hand side of the diagram.

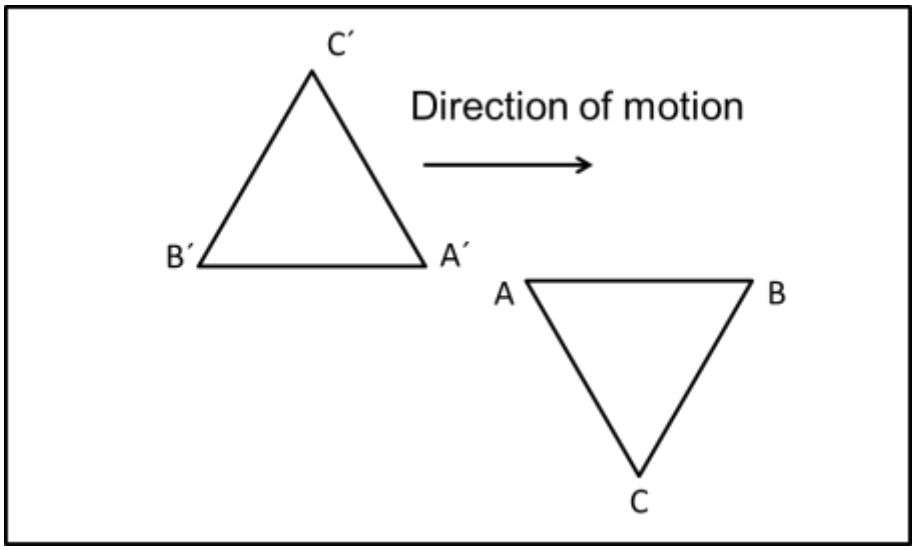

Fig. 4.5: Experimental set-up of experiments for observers with spatial geometry

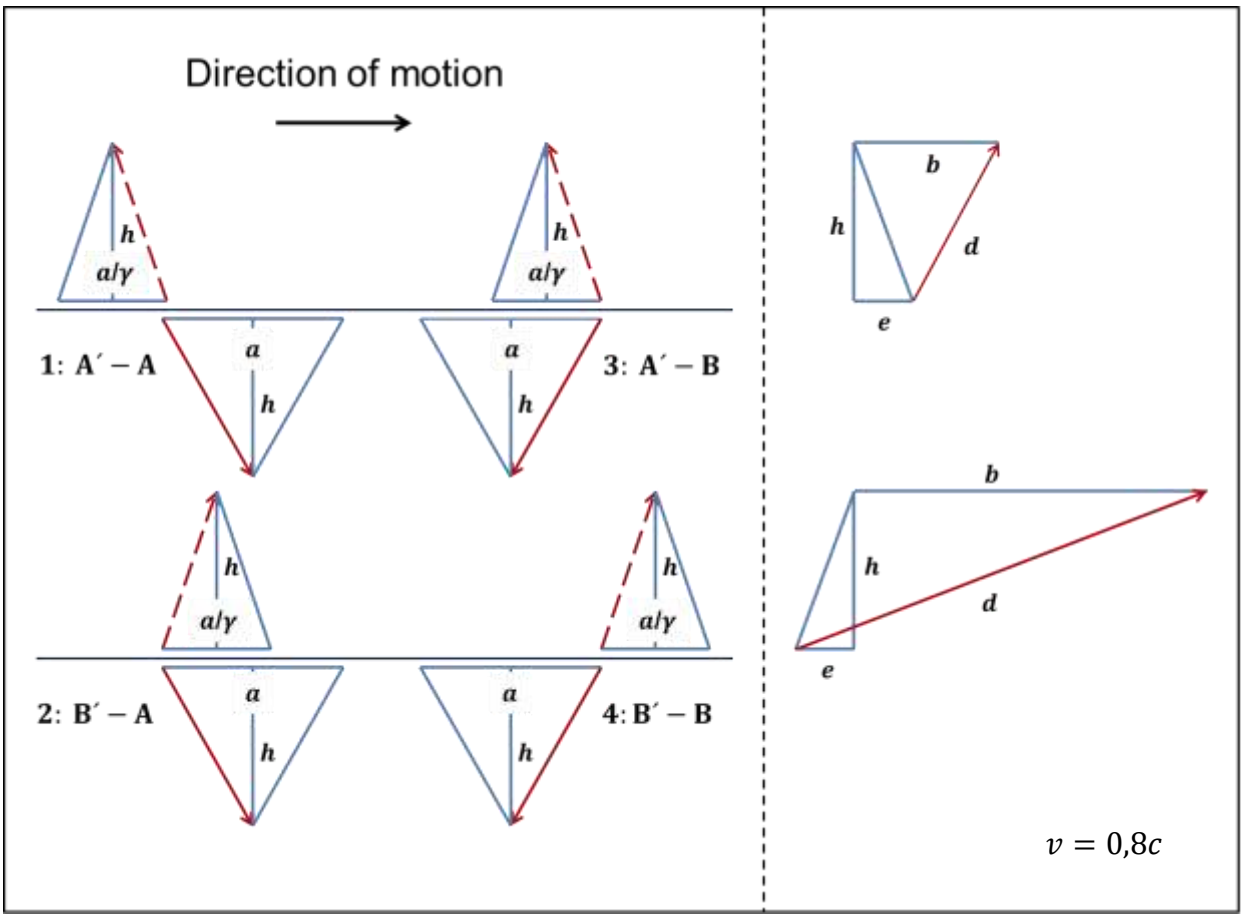

Fig. 4.6: Situation for contact and geometrical dependencies.

The geometrical dependency for distance d for cases 1 and 3 is defined by the Pythagorean theorem

$$(b-e)^2 + h^2 = d^2 \tag{4.40}$$

and with the relation

$$\frac{b}{d} = \frac{v}{c} \tag{4.41}$$

This leads to

$$\left(d\frac{v}{c} - \frac{a}{2\gamma}\right)^2 + \frac{3}{4}a^2 = d^2 \tag{4.42}$$

resulting in

$$d_{1/2} = -a\gamma\left(\frac{v}{2c} \pm 1\right) \tag{4.43}$$

If a signal is sent from B′ to C′ (cases 2 and 4) a slightly different approach is valid with

$$(b+e)^2 + h^2 = d^2 \tag{4.44}$$

and

$$d_{1/2} = a\gamma\left(\frac{v}{2c} \pm 1\right) \tag{4.45}$$

Only results with positive algebraic sign are permitted, so

$$\text{A}' \to \text{C}': \qquad \frac{d}{a} = \gamma\left(1 - \frac{v}{2c}\right) \tag{4.46}$$

$$\text{B}' \to \text{C}': \qquad \frac{d}{a} = \gamma\left(1 + \frac{v}{2c}\right) \tag{4.47}$$

If the value for time is standardized to 1 then

$$t_{\text{A}'\to\text{C}'} = \gamma\left(1 - \frac{v}{2c}\right) \tag{4.48}$$

$$t_{\text{B}'\to\text{C}'} = \gamma\left(1 + \frac{v}{2c}\right) \tag{4.49}$$

When the values for the returning signals are evaluated, it is instantly clear because of symmetry reasons

$$t_{C'\to B'} = t_{\text{A}'\to\text{C}'} = \gamma\left(1 - \frac{v}{2c}\right) \tag{4.50}$$

$$t_{\text{C}'\to A'} = t_{\text{B}'\to\text{C}'} = \gamma\left(1 + \frac{v}{2c}\right) \tag{4.51}$$

For a full calculation, the elapsing time between the contacts must be determined. When the time for contact A − A′ (case 1) is set to zero, then the following periods can be calculated using

$$\text{case1} \to \text{case2}: \qquad t_{1\to2} = \frac{c}{\gamma v} \tag{4.52}$$

$$\text{case1} \to \text{case3}: \qquad t_{1\to3} = \frac{c}{v} \tag{4.53}$$

$$\text{case1} \to \text{case4}: \qquad t_{1\to4} = \frac{c}{\gamma v} + \frac{c}{v} \tag{4.54}$$

With a suitable combination of these equations, it is possible to discuss the results of all situations of the experiment.

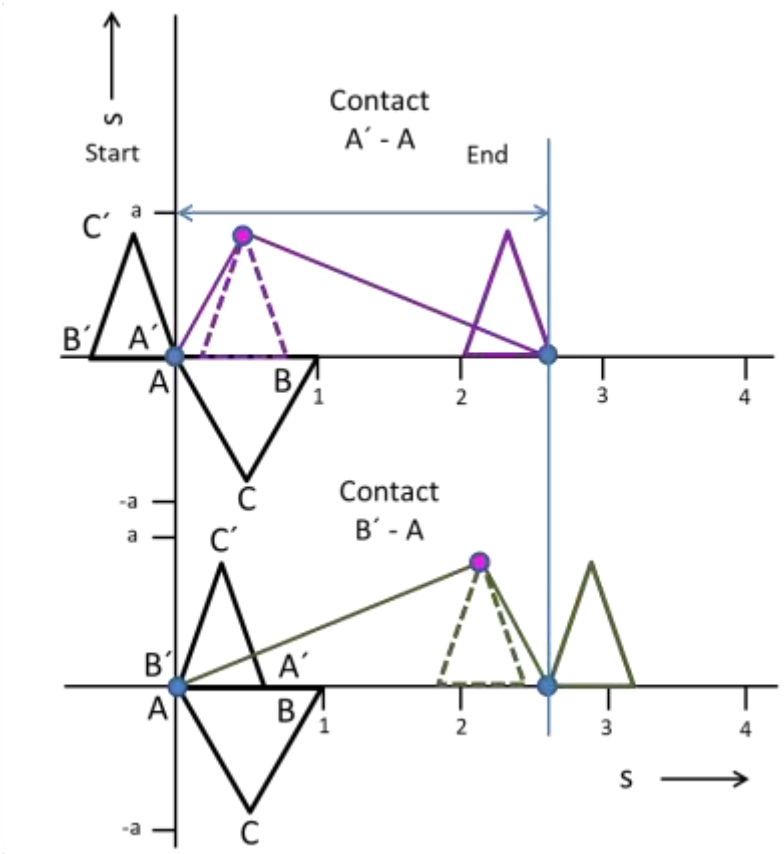

$v = 0{,}8c$

$A' - A$	System	System´
t_0	0	0
t_1	1	1
t_2	2	3,33

$B' - A$	System	System´
t_0	0,75	0,75
t_1	1,75	3,08
t_2	2,75	4,08

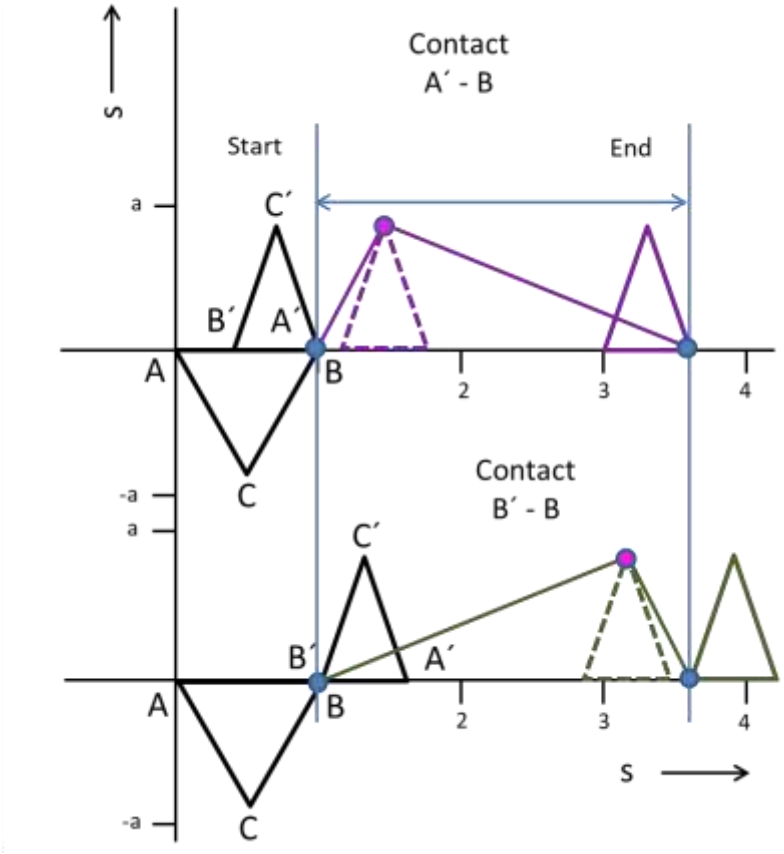

$A' - B$	System	System´
t_0	1,25	1,25
t_1	2,25	2,25
t_2	3,25	4,58

$B' - B$	System	System´
t_0	2	2
t_1	3	4,33
t_2	4	5,33

Fig. 4.7: Sequence of signals for the 4 possible contacts in the system.

In Fig. 4.7 the diagram for the experiment with a velocity of $v = 0{,}8\ c$ is presented. This high speed was chosen to provide an acceptable visual effect in the diagram, but this does not mean, however, that there are any restrictions in the universality of this relation.

For the 4 different contact situations the values for the total travelling time of signals sent from A′ resp. B′ to C′ and after reflection to their emitting points are added in the diagram. Furthermore, the equivalent measurements for the system presented by A, B, C are presented. To keep the evaluation simple the travelling time of a signal is standardized in a way that the distance a is set to 1. To make sure that the measurements can be compared with each other, the travelling times are adjoined by the times which elapsed since the sending of the first signal according to relations Eq. (4.52) to (4.54). The contact of A′ and A is representing the initial zero-value followed by B′/A, then A′/B and at last by B′ and B with $t = 2$.

According to the Theory of Special Relativity the "principle of identity" and after using the Lorentz Transformation the "principle of equivalence" must be valid. First it can be stated that the time for travelling the distance A→ C→ A and B→ C→ B is taking the total time $t = 2$, whereas for the distances A′→ C′→ A′ and B′→ C′→ B′ the time $t = 2.333 = 2\gamma$ is needed. This is exactly according to the anticipation valid for the situation of a moving observer.

When the time periods are considered, which are measured by C and C′ between the signals, then the same effect can be monitored, which was already discussed in chapter 2.2.2. This means, that the values of C and C′ for the contacts of A/B′ and B′/A are changing. It is obvious, that the principle of relativity requires, that C resp. C′ must receive the signal of the observer in their system A resp. A′ first. This is important to realize a proper sequence of contacts.

Generally, it was shown that all combinations sending signals in any arbitrary spatial direction are respecting the principle of relativity.

5.1 Signal exchange during rotation (Sagnac-effect)

In contrast to translational movements, there are measurable effects between outgoing and returning light beams in rotating systems. This does not contradict the principle of relativity, as by definition these are not inertial systems. The first successful experiments on this were carried out by Georges Sagnac (1860-1926) in 1913 [100].

The schematic experimental setup is shown in Fig. 4.8. Part a) shows that monochromatic light is emitted from a light source, which is partially reflected by a semi-transparent mirror and split into 2 opposing directions. After complete circulation and recombining, an interferometer is used to detect small transit time differences between the light beams. The apparatus is first calibrated at rest and then measurements are taken while the system is rotating. All elements of the experimental setup, i.e. light source, mirrors, and detector are also rotated. As shown in Fig. 4.8 b), the light beams emitted in the direction of rotation travel a longer distance than those moving in the opposite direction and this difference can be measured.

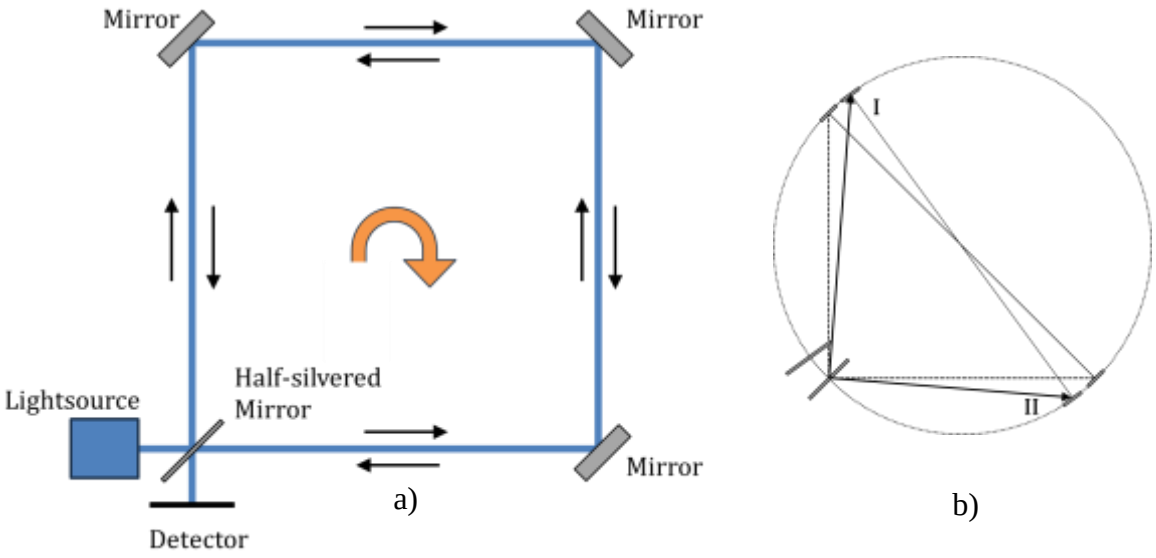

Fig. 4.8: Setup of a Sagnac interferometer. a) Rotatable test arrangement
b) Changing the measuring length of the first segment by rotation
Type I (in direction of rotation): Lengthening; type II (counter-rotating): Shortening

The designations shown in Fig. 4.9 can be used to calculate the values. The following relationship applies to the length of the arc segment s from A to B

$$s = r \cdot \omega \cdot (t_0 + \Delta t_0) \tag{4.60}$$

where r is the radius and ω is the angular frequency. In addition, t_0 is the time required by the light beam in the stationary system between 2 mirrors and Δt_0 is the additional time required for a rotational movement. The following also applies in general

$$a = ct_0 \qquad e = c\Delta t_0 \qquad b = a + e \qquad a = r\sqrt{2}$$

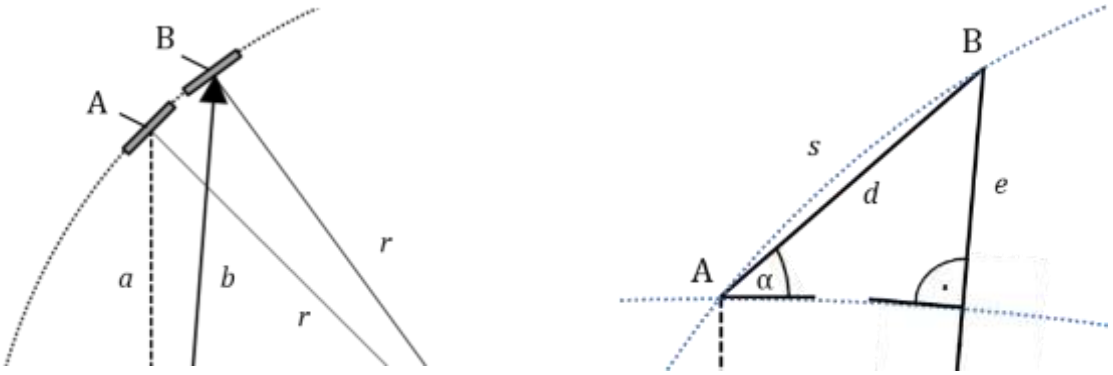

Fig. 4.9: Formula symbols used for the calculations

If $\Delta t \ll t_0$ is assumed, the following relationships apply as a good approximation

$$s = d = r \cdot \omega \cdot t_0 \tag{4.61}$$

$$\sin\alpha = \sin(45°) = \frac{1}{\sqrt{2}} = \frac{e}{d} = \frac{c \cdot \Delta t_0}{r \cdot \omega \cdot t_0} \tag{4.62}$$

and thus

$$\Delta t_0 = \frac{r\omega t_0}{\sqrt{2}\cdot c} = \frac{a^2\omega}{2c^2} \tag{4.63}$$

There are 4 segments, so the time delay for one cycle is

$$\Delta t_+ = 2\frac{a^2\omega}{c^2} \tag{4.64}$$

The shortening of the time for the light beam on the opposite path has the same value, so the final result is

$$\Delta t_t = \Delta t_+ + \Delta t_- = 4\frac{a^2\omega}{c^2} \tag{4.65}$$

With a length a of 1m and 10 revolutions per second, this results in $\Delta t_t = 4{,}4 \cdot 10^{-16}$s corresponding to a wavelength in visible light that allows interference measurements.

G. Sagnac was convinced that he had measured an ether effect with his (similarly constructed) apparatus; however, Max v. Laue had already demonstrated in 1911 that such an experiment was compatible with the principle of relativity [101].
In 1925, A. A. Michelson and H. G. Gale carried out an experiment with dimensions of 613 m in length and 339 m in width [102,103]. This made it possible to measure the rotation of the earth with a relative accuracy of 2%.

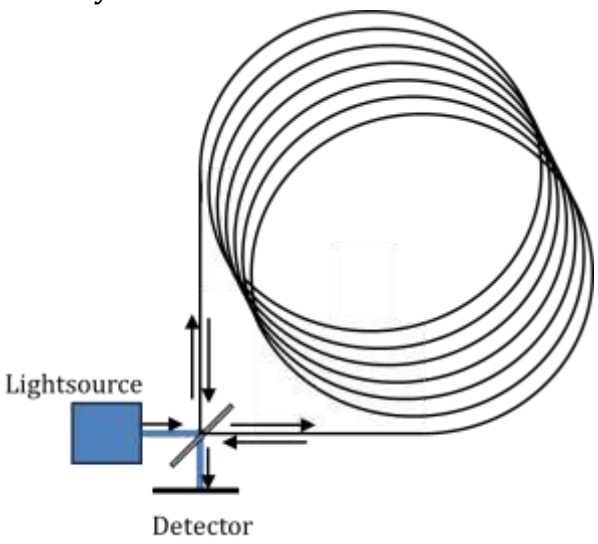

Fig. 4.10: Construction of a Sagnac interferometer with an optical fiber

In addition to the structure with beam reflection by mirrors, coiled fiber optic cables can also be used as shown in Fig. 4.10. These are widely used today in areas such as aerospace, navigation, ships, and robotics. They are less susceptible to mechanical wear than mechanical gyrocompasses as they contain no moving parts. Another trend in their development is the miniaturization of optical gyroscopes. With the advent of micro-electro-mechanical systems (MEMS), it has become possible to produce smaller and more cost-efficient gyroscopes that can be used for a variety of applications, from smartphones to drones.